PHYSICAL REVIEW B VOLUME 27, NUMBER 1 1 JANUARY 1982

Static and dynamic properties of one-dimensional disordered magnetic Ising Systems

Jorge V. José
*Instituto de Física, UNAM, Apartado Postal 20-364, Mexico 01000, D.F., Mexico and Physics Department, Northeastern University, Boston, Massachusetts 02115**

Michael Mehl†
Physics Department, Rutgers University, Piscataway, New Jersey 08854

Jeffrey B. Sokoloff
Physics Department, Northeastern University, Boston, Massachusetts 02115
(Received 1 February 1982; revised manuscript received 7 May 1982)

The Ising model with random nearest-neighbor couplings is studied numerically and analytically. The J's are chosen to obey the probability laws $P(J)\sim |J|^{-\alpha}$ with $0<\alpha<1$, $-1<J<0$ for AF, $0<J<1$ for F, and $-1<J<1$ for SG. Here F means ferromagnetic, AF indicates antiferromagnetic, and SG stands for spin-glass. The thermodynamic properties are evaluated for arbitrary temperature, magnetic field, and α. The dynamics is defined by a Glauber equation of motion with random hopping matrices $\Gamma^{+}(J_i,J_{i-1})$, $\Gamma^{-}(J_i,J_{i-1})$, and $\Gamma^{+}(J_i,J_{i-1})=\Gamma^{-1}(J_{i-1},J_i)$. We use a continued-fraction method to evaluate the quenched averaged magnetization with M as a function of time. We find that M has two components: a fast one M_F that decays exponentially and a slow nonuniversal nonexponential one M_r. A new type of clusters, named Γ clusters, are found to be responsible for the existence of M_r, as well as the fact that $P_0(J)$ should be a *continuous* function of J. In the case for which the J's take only discrete values, $M_r=0$. This result is obtained analytically and checked numerically via a Monte Carlo simulation of the model. The appearance of M_r is found to depend strongly on initial conditions. In particular for the AF case when all spins are parallel initially $M_r=0$. Hysteresis loops for the F, AF, and SG cases are also obtained with the Monte Carlo method. We point out that our results for the AF case are qualitatively similar to the recent dynamic experiments on quinolinium-di-tetracyanodimethanide complexes.

I. INTRODUCTION

A significant advance has been made recently in the understanding of the *static* properties of magnetic chains with random antiferromagnetic exchanges.[1-5] The model Hamiltonians studied are of the isotropic Heisenberg form

$$H=\sum_i J_i\vec{S}_i\cdot\vec{S}_{i+1}-\sum_i \vec{h}\cdot\vec{S}_i \ . \tag{1}$$

Here J_i is the nearest-neighbor random exchange and $\vec{h}$ is an externally applied magnetic field. Two distinctive limits can be studied depending on the nature of the spin operators $\{\vec{S}\}$. When the magnitude of the spin is "infinite" the operators are unit vectors. This is the classical limit. The other limit is when the magnitude of the spin operators is $\frac{1}{2}$. This is the quantum limit and the operators are the Pauli-spin-$\frac{1}{2}$ operators. A lot of the interest in studying these models has been due to the experimentally realizable quantum limit found in charge-transfer complexes.[1] One of the most striking recent findings is that the random-classical and quantum cases belong to different universality classes.[2] The definition of universality classes here is related to the probability law for J_i, $P(J_i)$. It was found that the thermodynamics of the quantum case is independent of the form of $P(J_i)$. In contrast, in the classical n-vector models and the $s=\frac{1}{2}$ Heisenberg random ferromagnet the results depend strongly on $P(J_i)$.[6] The currently known members of the quantum class are the model given in Eq. (1) together with anisotropic (X-Y) Heisenberg antiferromagnetic (AF) models. The quantum universality class predictions have been nicely confirmed experimentally by Clark and collaborators.[1]

With regard to the dynamic properties of these models almost nothing is known. One of the

reasons for this is, of course, that dynamic studies are more difficult than static ones. In this paper we study the dynamic properties of one of these models: the Ising model with singular $P(J)$. The physical motivation for taking $P(J)$ singular will be given later. For reasons of completeness and of furthering our understanding of the dynamic properties of the random Ising model we study the antiferromagnet, as well as the ferromagnetic (F) and spin-glass (SG) cases. Also in Sec. II we present a unified study of the thermodynamic properties of these models for arbitrary temperatures and magnetic fields that are helpful in the dynamic studies. Some of these results are already known.

The dynamic model studied in Sec. III of this paper is defined by the equation of motion

$$\frac{dq_i}{dt} = -q_i + \Gamma_i^+ q_{i+1} + \Gamma_i^- q_{i-1} \,. \tag{2}$$

This is just Glauber's[7] equation extended to random J's. Here q_i is the thermally averaged on-site magnetization. The new items introduced by the random J's are the hopping matrices $\Gamma^{\pm}$ that are no longer symmetrical. The Γ functions depend on two J's, i.e., J_i and J_{i-1}, and satisfy $\Gamma^+(J_i,J_{i-1}) = \Gamma^-(J_{i-1},J_i)$. Their explicit form will be given in Sec. III. We notice that Eq. (2) has the same form as the Laplace transformed tight-binding Hamiltonian equation of motion, studied in electronic problems with off-diagonal disorder. Here the lack of symmetry of the Γ's makes the problem somewhat more complicated. As we discuss in Sec. III C in an intermediate-temperature region the asymmetry is weak and the two disordered problems are analogous. The tight-binding problem with off-diagonal disorder has been studied extensively. It is found that the density of states has a singularity at the center of the band. This singularity, however, is integrable and does not lead to any measurable quantity in our problem.

One of our main goals is to calculate the quenched averaged magnetization $M = [\tilde{M}(J,t)]_J$. The square brackets mean averaging with respect to $P(J)$. We choose the form of $P(J)$ based on two physically plausible conditions: randomly located agnetic moments and interactions that decay exntially with distance. These two assumptions [8]

$$\cdot(1-\alpha)/J^{\alpha} \,. \tag{3}$$

of J are bounded $(0 < J \leq 1)$ and re complete discussion of this probven in Sec. II. We use the ethod to evaluate $M(t)$ analyti- $M(t)$ has two components, a fast one, M_f, that decays exponentially with time, and a slow nonexponential time decay. Here we find first that there is remanence in all three cases (AF,F,SG). The amount of remanence depends strongly on the value of α, therefore on $P(J)$. The remanence is largest in the F case and smallest in the AF case. At $T=0$ all models have remanence, however, irrespective of the form of $P(J)$ *provided* $P(J)$ *is a continuous function of* J. Specifically, we find that

$$M_r \sim \tfrac{1}{3} - f(\alpha)(T\ln t) - g(\alpha)(T\ln t)^{3(1-\alpha)} + \cdots \,, \tag{4}$$

with $T\ln t \ll 1$. For $0 \lesssim \alpha \lesssim 0.5$, the third term is irrelevant and the $T\ln t$ dominates. However, for $0.8 \lesssim \alpha < 1$ the dominant contribution is proportional to $(T\ln t)^{3(1-\alpha)}$. For intermediate values of α the two $(T\ln t)$ terms contribute and the explicit forms of $g(\alpha)$ and $f(\alpha)$ are given in Sec. III.

We also find that in the AF case the remanence is strongly dependent on the initial conditions and is zero if the initial state is fully magnetized. In Sec. IV we give supporting arguments of why this is so and confirm them via a Monte Carlo (MC) simulation. There we start at high temperatures in the presence of a field. Then we lower the temperature in the usual MC way to reach the desired temperature and then turn off the field and observe how the magnetization relaxes to zero. With the MC method we are also able to calculate other quantities of interest which seem much harder to calculate analytically. In particular we have looked at the hysteresis loops. Their shapes are in agreement with the changes in M_r seen in the thermoremanent measurements and the analytic results. We also compare our analytic results with the numerical continued-fraction results of Ref. 9.

In brief, Sec. II deals with the thermodynamics of the three cases F, AF, and SG for arbitrary temperatures, field, and α. This includes as well a discussion of three different static correlation lengths that can be defined in random systems. In Sec. III the Glauber model is solved exactly at $T=0$ and approximately for low, intermediate, and high temperatures. Here a new type of clusters named Γ clusters is found to be responsible for the existence or remanence in these models. In Sec. IV the Monte Carlo method is used to help in furthering our understanding of the random Ising model in the presence of a field for different T's and α's. Finally in Sec. V we collect the main results of the paper and discuss their possible relevance to the dynamic experiments performed on quinolinium-ditetracyanodimethanide [Qn(TCNQ)$_2$] by Clark and his collaborators.[10] Part of the results of this paper

pertaining to the AF case have been communicated briefly elsewhere.[11,12]

II. STATIC PROPERTIES

In this section we discuss the thermodynamic properties of the Ising random chains defined in Sec. I. The idea of clusters has been helpful and widely used in the study of random magnetic systems. Here we begin by discussing the properties of $P(J)$ itself. This leads to the definition of percolation clusters associated with $P(J)$. Then we go on to discussing the thermodynamic properties in the absence of a magnetic field for the F, AF, and SG Ising chains. Here we complete the analytic low-temperature results for arbitrary temperatures by using a numerical evaluation of the partition function. The thermal correlation length that leads to the definition of thermal clusters and the "scaling" correlation length are obtained in Sec. II C. In Sec. II D the magnetic field properties for small and large h are obtained analytically and the intermediate region numerically.

A. The probability law

The average strength of the J's depends on the value of α. For α small, on the average, the couplings are stronger ($J\sim 1$) than when α is large where most of the couplings are weak ($J\sim 0$). This is easily seen from a computer-generated plot (Fig. 1) based on Eq. (3), for $\alpha=0.3$, 0.7, and 0.9. A more quantitative description of the relevance of the magnitude of the J's comes from comparing them with the temperature T. The coupling between two adjacent spins is considered strong if $J>T$ and weak if $J<T$. The probability that an arbitrary J is weak is $\sim T^{1-\alpha}$. The probability of having a cluster of $L+1$ strongly connected spins separated from the rest of the lattice by weak couplings on both ends is

$$T^{2(1-\alpha)}e^{L\ln(1-T^{1-\alpha})} .$$

On the average then, L adjacent spins are strongly coupled if $L\lesssim\xi_\alpha(T)$, where

$$\xi_\alpha^{-1}=-\ln(1-T^{1-\alpha}) . \tag{5}$$

We call ξ_α the percolation correlation length. Of course, this definition of cluster is the usual one, which we call J clusters, and was first used for these types of problems by Theodorou and Cohen.[8] Here we want to compare $\xi_\alpha(T)$ with the thermal correlation length characteristic of the Ising model. Also we will compare the J clusters with the Γ clusters to be defined in Sec. III, which depend on the relative magnitudes of successive J's, and are responsible for the appearance of remanence in these models.

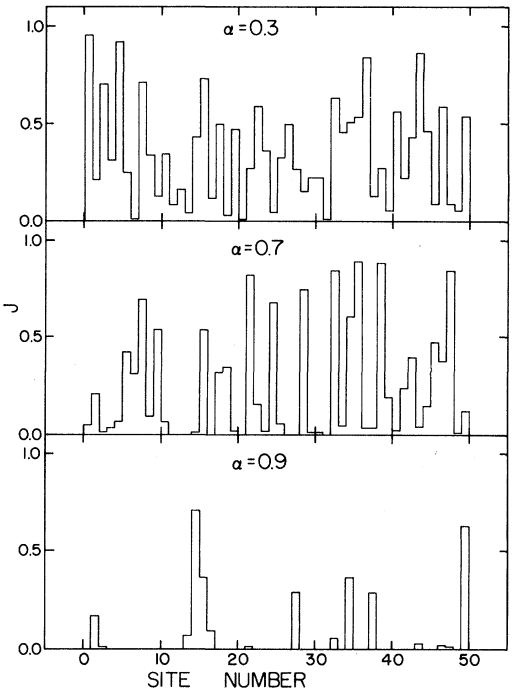

FIG. 1. Small portions of the lattices generated using the probability distribution given by Eq. (3) with $\alpha=0.3$, 0.7, and 0.9.

B. Thermodynamic quantities

In zero field the thermodynamics of these models are calculated straightforwardly for arbitrary $P(J)$. The specific heat is given by[13]

$$C_\alpha(T)=\int P(J)(J/T)^2\mathrm{sech}^2(J/T)dJ , \tag{6}$$

whereas the susceptibility χ at zero field reads

$$T\chi_\alpha(T)=[1-\rho_\alpha(T)]/[1+\rho_\alpha(T)] \tag{7}$$

with

$$\rho_\alpha(T)=\int P(J)\tanh J/T\,dJ . \tag{8}$$

The AF model is defined in terms of $P(J)$ given in Eq. (3). For the F case we take

$$P^{\mathrm{F}}(J)=(1-\alpha)|J|^{-\alpha} , \tag{9}$$

with $-1\le J\le 0$, and the SG case by

$$P^{\mathrm{SG}}(J)=\tfrac{1}{2}(1-\alpha)|J|^{-\alpha} , \tag{10}$$

where $0<|J|\le 1$. We note that $C_\alpha^{\mathrm{AF}}=C_\alpha^{\mathrm{F}}=C_\alpha^{\mathrm{SG}}$, because C_α is an even function of J. On the other hand,

$$\chi_\alpha^{\mathrm{F}}(T)=T^{-2}[\chi_\alpha^{\mathrm{AF}}(T)]^{-1} , \tag{11}$$

and for the SG case[14]

$$\chi_\alpha^{\mathrm{SG}}(T)=1/T\ , \tag{12}$$

independent of α. At low temperatures $C_\alpha(T)\sim T^{1-\alpha}$ and $[1-\rho_\alpha(T)]\sim T^{1-\alpha}$, which implies that

$$\chi_\alpha^{\mathrm{AF}}(T)\sim T^{-\alpha}\ . \tag{13}$$

This behavior for χ is also obtained for the $s=\frac{1}{2}$ Heisenberg AF but for arbitrary $P(J)$ and with α weakly dependent on T. Here the result is inherently related to the form of $P(J)$. From Eq. (11) it follows that

$$\chi_\alpha^{\mathrm{F}}(T)\sim T^{\alpha-2}\ , \tag{14}$$

which is also divergent and an explicit function of α. A result of this kind does not seem to have been seen yet experimentally.

The region of validity of Eq. (13) can be found numerically. We find that for temperatures smaller than 0.1 the low-T result is essentially valid, as can be seen from Figs. 2 and 3. It is essentially *below 0.1* where we find remanent effects in the AF model in Sec. IV. At high temperatures $C_\alpha\sim T^{-2}$ and $\chi_\alpha\sim T^{-1}$ as they should.

C. Static correlation functions

Another quantity of interest at zero field is the thermal correlation length $\xi_T(\alpha)$, which measures the average distance at which two spins are correlated. The quenched average spin-spin correlation function between a spin at the origin and one a distance n away is

$$(\langle S_0S_n\rangle)_J=e^{-n/\xi_T(\alpha)}\ . \tag{15}$$

The correlation length is given by the equation

$$\xi_T^{-1}(\alpha)=-\ln(\tanh J/T)_J\ . \tag{16}$$

Recently there have seen some suggestions that the right quantity to average is not necessarily the correlation function itself but the averaged logarithm of $\langle S_0S_n\rangle$.[2,15,16] In our case this becomes

$$(\ln\langle S_0S_n\rangle)_J=n\,(\ln\tanh J/T)_J\ , \tag{17}$$

which leads us to define the scaling correlation length by

$$\xi_{\mathrm{sc}}^{-1}=-(\ln\tanh J/T)_J\ .$$

At sufficiently low temperatures $\xi_\alpha^{-1}(T)$, $\xi_T^{-1}(\alpha)$, and ξ_{sc}^{-1}, except for numerical factors of $O(1)$, go like $T^{1-\alpha}$. At higher temperatures they differ in behavior as can be seen from the plots of ξ_α, ξ_{sc}, and $\xi_T(\alpha)$ in Fig. 4. Here we are interested in the low-temperature limit of the problem and therefore conclude that using the average given in Eq. (15) or (17) leads to essentially the same results, contrary to what was found in the examples considered in Ref. 16. In particular, the fluctuation dissipation theorem can be used to derive Eq. (7) with either of the two averages. It is possible, however, that when calculating the dynamic correlation functions this equivalence will not hold and a representative average for the ensemble has to be found. In Sec. III we define another correlation length related to the dynamical properties of these models at intermediate temperatures.

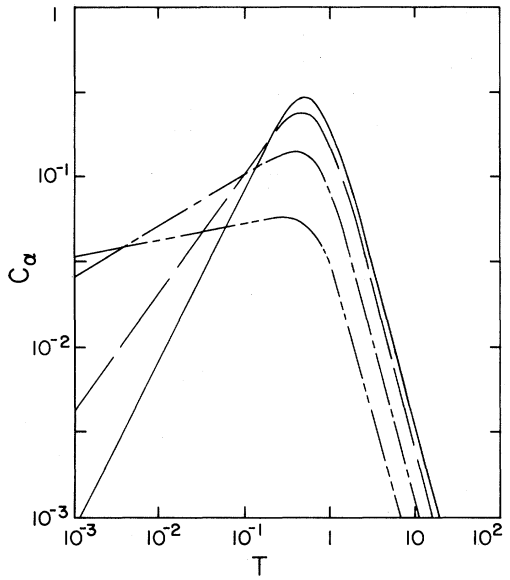

FIG. 2. Specific heat given in Eq. (6) for different values of α as a function of temperature. This plot shows $\alpha=0$ (——), $\alpha=0.3$(—), $\alpha=0.7$(— - — - —), and $\alpha=0.9$(— - — - — - —). C_v is the same for ferro-, antiferromagnetic and spin-glass cases.

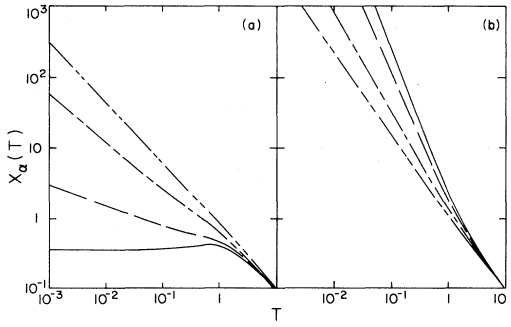

FIG. 3. Zero-field magnetic susceptibility, Eq. (7), for (a) antiferromagnet and (b) ferromagnet. The curves for different α's are the same as in Fig. 2. The graphs are given in a log-log scale.

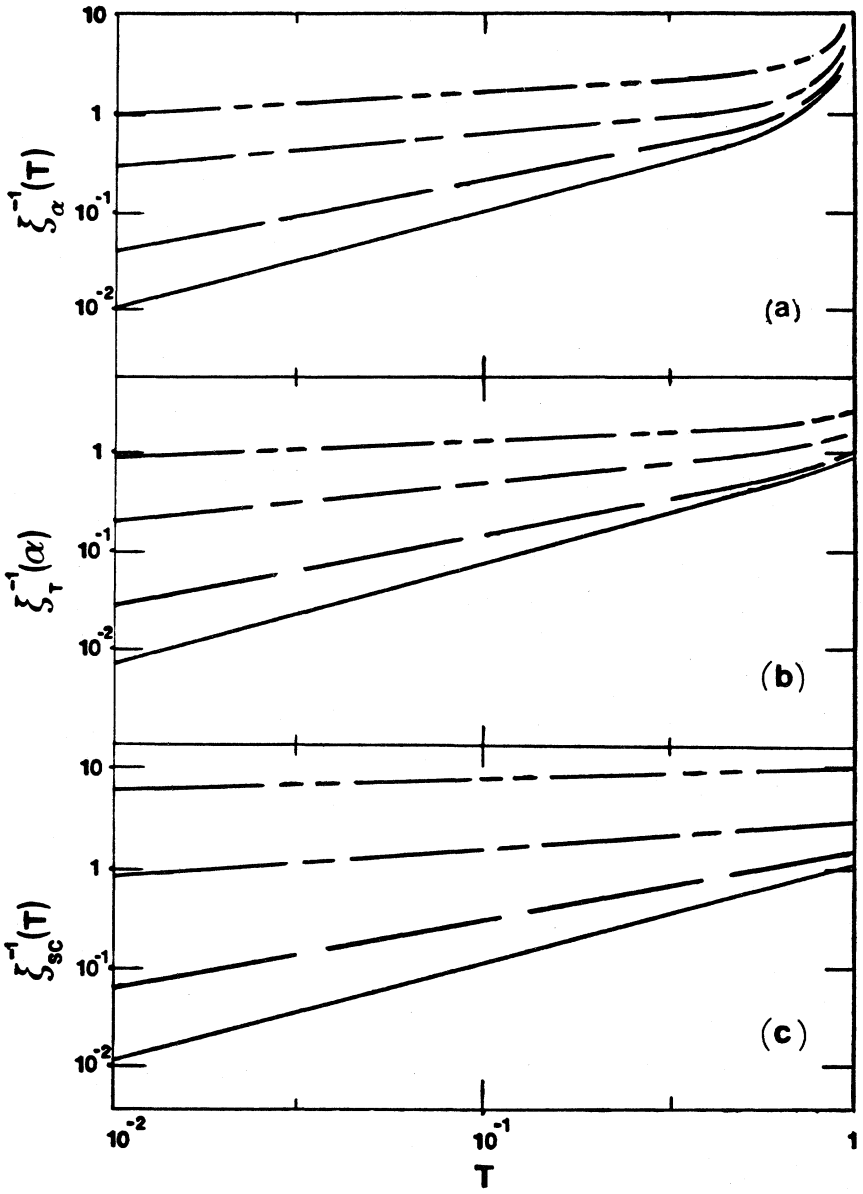

FIG. 4. (a) Inverse percolation length [Eq. (5)] for $T<1$, (b) inverse thermal correlation length [Eq. (16)], and (c) inverse scaling length. The classification of curves for different α's is the same as in Fig. 2.

D. Field-dependent results

The equilibrium properties for $\vec{h}\neq 0$ cannot be evaluated exactly. In fact, there is a large body of literature treating this problem with both $\vec{h}$ and J random.[17] Here we will be content with obtaining asymptotic expressions for large and small $\vec{h}$ and will connect both expansions numerically. In the small-$\vec{h}$ limit the free energy is

$$[F_\alpha(T,h)]_J=[F_\alpha(T,h=0)]_J - \tfrac{1}{2}\chi_\alpha(T)h^2+O(h^4)\ , \tag{18}$$

where $\chi_\alpha(T)$ is given in Eq. (7). The next order correction is more complicated and involves the four-point correlation function calculation. The high-h limit gives

$$(F_\alpha)_J=-h-[4(1-\alpha)/T]e^{-2(h-2)/T}+\cdots\ , \tag{19}$$

which is valid for $T\ll 1$ and $h>2$. The intermediate region is calculated using a numeric evaluation of the free energy as a function of h. Specifically, we take a set of J's chosen according to the probabil-

ity law given in Eq. (3). Then we evaluate a product of N transfer matrices that gives $[F_\alpha(T,h)]_J$. This free energy is numerically differentiated with respect of h to obtain the equilibrium magnetization shown in Fig. 5. These results are compared and used to normalize the Monte Carlo results presented in Sec. IV.

III. DYNAMIC PROPERTIES

In this section the kinetic equation of motion with random bonds is studied. We start by analyzing the $T=0$ properties of the solutions. In this limit the hopping matrices take numerical values that permit an explicit solution of the equations in terms of the new type of clusters called Γ clusters, which are responsible for the appearance of remanence. In the Γ_1 clusters the magnitude of successive J's increase whereas those of the Γ_2 clusters decrease as one goes from left to right. The solutions are obtained for the F, AF, and SG cases in this limit, and their similarities and differences are discussed. Next the quenched averaged magnetization is calculated at finite but low temperatures. This is done using the standard continued-fraction method to solve finite difference equations. A discussion of the intermediate-temperature regime is also presented. Here the equation of motion is essentially of the type studied in the random electronic problem via the tight-binding Hamiltonian with off-diagonal disorder studied by several authors. The high-temperature limit is trivial and corresponds to diffusive-type solutions for the magnetization.

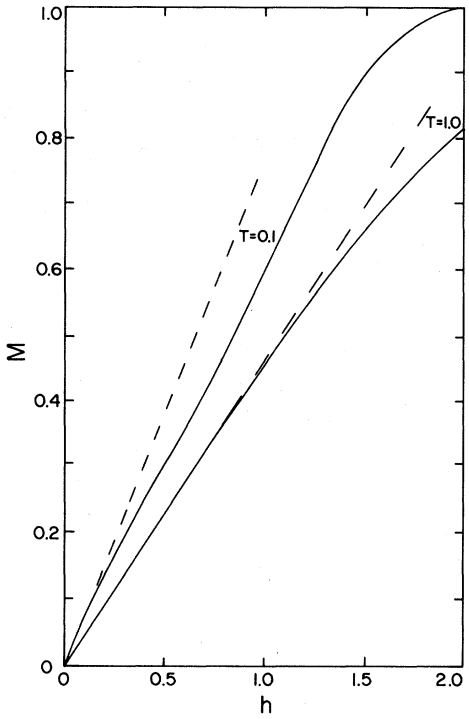

FIG. 5. Exact magnetization as a function of the field h and temperature T for a 1001 spin lattice with $\alpha=0.3$. The method of calculation is described in the text. The dashed lines are the functions $\chi_{0.3}(T)h$, when $\chi_{0.3}(T)$ is obtained from Eq. (7).

A. Equation of motion

The Glauber equation of motion is a master equation with single spin flips induced by a thermal reservoir located at each lattice site. From the detailed balance condition we have

$$\frac{\omega_i(S_i)}{\omega_i(-S_i)}=\frac{1-S_i\tanh E_i/T}{1+S_i\tanh E_i/T}\ ,$$

where $S_i=\pm1$, ω_i gives the probability of a single spin flip, and $E_i=J_{i-1}S_{i-1}+J_iS_{i+1}$. The equation of motion reads

$$\frac{dq_i(t)}{dt}=-q_i+\langle\tanh E_i/T\rangle\ . \tag{20}$$

Here we have taken the same relaxation time for all the spins in the chain, and equal to one. q_i is the thermally averaged on-site magnetization for a given configuration of J's defined by

$$q_i(\{J_i\})=\sum_{\{S\}}S_iR(\{S\},\{J\},t)\ ,$$

with R being the probability density. The thermally averaged $\tanh E_i/T$ can be written immediately as

$$\tfrac{1}{2}[\tanh(J_i+J_{i-1})/T+\tanh(J_i-J_{i-1})/T]q_{i+1} \tag{21}$$

$$+\tfrac{1}{2}[\tanh(J_i+J_{i-1})/T-\tanh(J_i-J_{i-1})/T]q_{i-1}\ , \tag{22}$$

which allows us to write (20) as

$$\frac{d}{dt}q_i=-q_i+\Gamma_i^+q_{i+1}+\Gamma_i^-q_{i-1}\ ,$$

where Γ^+ and Γ^- are the coefficients of q_{i+1} and q_{i-1} given in Eq. (21) and Eq. (22), respectively. The Laplace transform of this equation gives

$$(1+s)\tilde{q}_i=\Gamma_i^+\tilde{q}_{i+1}+\Gamma_i^-\tilde{q}_{i-1}+q_i(0) \tag{23}$$

with

$$\tilde{q}_i(s)=\int e^{st}q_i(t)dt\ .$$

B. $T=0$ solutions

Equation (23) acquires a simple form at zero temperature because the Γ functions take only the values 0, ± 1, and $\pm\frac{1}{2}$. We start by considering the F and AF cases and the SG case at the end. When $|J_i| > |J_{i-1}|$, $\Gamma_i^+=\eta$, and $\Gamma_i^-=0$, with $\eta=1$ for F and -1 for AF. The region in the chain $n_1 \le i \le n_2$ with $|J_{n_2}| > |J_{n_{2-1}}| > \cdots > |J_{n_1}|$ has $\Gamma_i^+=\eta$ and $\Gamma_i^-=0$. We call this section of the chain a Γ_1 cluster. Similarly, if $|J_i| < |J_{i-1}|$, $\Gamma_i^+=0$, and $\Gamma_i^-=\eta$, and for $|J_{n_2}| < |J_{n_{2-1}}| < \cdots < J_{n_1}|$ with $n_i \le i \le n_2$ define the Γ_2 clusters. When $|J_{n_2}| = |J_{n_{2-1}}| = \cdots + |J_{n_1}|$, $\Gamma_i^+=\Gamma_i^-=\frac{1}{2}\eta$ and this segment of the chain is called a Γ_3 cluster. As will be seen in this section the remanent properties associated with the (Γ_1,Γ_2) clusters are physically different than those of the Γ_3 clusters. In fact, the Γ_3 clusters do not lead to remanence. Also, because the $P(J)$ of interest in this paper is continuous, the likelihood of having Γ_3 clusters is smaller than that for (Γ_1,Γ_2) clusters and we study the latter type of clusters first. Equation (23) at $T=0$ reads

$$\epsilon\tilde{q}_i(s)=\eta\tilde{q}_{i+\delta}(s)+q_i(0) . \tag{24}$$

Here $\delta=1$ for a Γ_1 cluster and $\delta=-1$ for a Γ_2 cluster, with $\epsilon=s+1$. Consider the sites $n_1<n<n_2$ such that the magnitude of the J's are in ascending magnitude for $n_1<i\le n$ and descending for $n<i<n_2$. Equation (24) for $i=n$ and $n+1$ can be solved for $\tilde{q}_{n+1}(s)$ giving[12]

$$\tilde{q}_{n+1}(s)=\frac{1}{s(s+2)}[(1+s)q_{n+1}(0)+\eta q_n(0)] . \tag{25}$$

The relevant pole in this equation is at $s=0$, because when Eq. (25) is inverse Laplace transformed it leads to a constant when $t\to\infty$, whereas the $s=-1,-2$ poles lead to exponential decay with time. Note that this result reveals an important physical difference between the F and AF cases. In the F case there will be remanence regardless of the initial conditions $\{q_i(0)\}$ chosen, except, of course $\{q_i(0)=0\}$ and $q_i(0)=(-1)^i$, which is an AF type of initial condition. In contrast, in the AF case in order to have remanence the set $\{q_i(0)\}$ should not be the same for all i. In particular, the case of all spins aligned by a strong magnetic field should lead to zero remanence. These results are confirmed in Sec. IV by an explicit Monte Carlo sampling evaluation of the magnetization.

For a given i the residue of $\tilde{q}_i(s)$ at $s=0$ is given by

$$\mathrm{Res}[\tilde{q}_i(s)]=\tfrac{1}{2}\eta^{|i-n|}[q_n(0)+\eta q_{n+1}(0)] . \tag{26}$$

It should be noted that the value of $\tilde{q}_i(s)$ for $i<n_1$ or $i>n_2$ is not related to $\tilde{q}_i(s)$ for $n_1\le i\le n_2$. This result implies that the chain may be divided into clusters which we will refer to as $(\Gamma_1+\Gamma_2)$ clusters. For example, the region $n_1\le i\le n_2$ is such a cluster. It is characterized by an increase in magnitude of successive J values up to a maximum value, followed by a decrease as we move from left to right through the chain. From what we have just said, successive $(\Gamma_1+\Gamma_2)$ clusters are uncoupled. This occurs because each spin always tries to satisfy the stronger of its two bonds at $T=0$. *We believe that these clusters are responsible for the observed remanence.* From Eq. (26), we also see that only odd clusters will contribute to the remanence in the antiferromagnetic case.

In the SG problem both positive and negative exchanges are allowed at random. We can again define coupled Γ clusters in which the magnitude of the J's to the left of J_n increases and the couplings to the right of J_n decrease in magnitude as well. The equation of motion in this case can be solved as in the F and AF cases. The differences can be seen by considering the absolute value of the solution given in Eq. (26),

$$|\,\mathrm{Res}\tilde{q}_i(s)\,| = |\,q_n(0)+\eta q_{n+1}(0)\,| , \tag{27}$$

where $\eta=1$ if $J_n>0$ and $\eta=-1$ if $J_n<0$. Because, again, the residue depends on the stronger coupling the signs of the J's can switch to the right or to the left of J_n but the absolute value of the residue will not change. The $\mathrm{Res}\tilde{q}_i(s)$ itself will alternate signs in an AF-coupling region and will remain with the same sign in a F segment, however. Thus we see that the physical reasons for the appearance of the remancence in the three cases, F, AF, an SG is the same. Note that *the results at $T=0$ are independent of $P(J)$ provided the distribution is continuous for each case.*

Finally, we consider the Γ_3 clusters at $T=0$. The equation of motion in this case is

$$\frac{d}{dt}q_i=-q_i+\tfrac{1}{2}\eta(q_{i+1}+q_{i-1}) . \tag{28}$$

This equation can be solved by different methods including the one used by Glauber with appropriate boundary conditions. A similar analysis to the one given above, however, shows that the $s=0$ pole does not appear and only exponential decays with time within a given cluster are found. The results of this section explain why calculations with discrete proba-

bility distribution functions[18] have very different long-time properties.

C. Low-temperature regime

Armed with the understanding gained in the preceding section we can proceed to calculate the averaged magnetization at low temperatures. At nonzero temperatures the remanent magnetization decays slowly with time. The manner in which the decay takes place can be found from the expression for the averaged magnetization

$$M(t)=\frac{1}{2\pi i}\int_{-i\infty+\delta'}^{i\infty+\delta'} ds \sum_{l,k}[G_{l,k}(s)]_J q_k(0)\rho^{st} . \tag{29}$$

Here $i=\sqrt{-1}$ and $G_{l,k}$ is the Green's function associated with Eq. (23). $G_{l,k}$ can be calculated using the standard continued-fraction method. At low temperatures we are interested in the low-order pole structure of $G_{l,k}$. At $T=0$, $G_{l,k}(s)$ has a pole at $s=0$ as for the q_i given in Eq. (25). Following Ref. 19, we find that the poles of $G_{l,k}(s)$ occur when

$$s+1-\cfrac{\beta_l^+}{(s+1)-\cfrac{\beta_{l+1}^+}{(s+1)+\cdots}}-\cfrac{\beta_{l-1}^-}{(s+1)-\cfrac{\beta_{l-z}^-}{(s+1)+\cdots}}=0 , \tag{30}$$

where $\beta_l^{\pm}=\Gamma_l^{\pm}\Gamma_{l\pm1}^{\mp}$. In the asymptotic limit of low temperatures, we may expand the β's to lowest order. Consider the following cases:

(a) $J_{l-1}>J_l>J_{l+1}$,

(b) $J_{l-1}<J_l>J_{l+1}$,

(c) $J_{l-1}>J_l<J_{l+1}$,

(d) $J_{l-1}<J_l<J_{l+1}$.

For each of these four cases $\beta_l^{\pm}$ is given approximately by

$$\begin{aligned} &e^{-(J_{l-1}-J_l)/T}-e^{-(J_{l-1}-J_{l+1})/T} ,\\ &1-e^{-(J_l-J_{l-1})/T-(J_l-J_{l+1})/T} ,\\ &e^{-(J_{l+1}+J_{l-1}-2J_l)/T} ,\\ &e^{-(J_{l+1}-J_l)/T}-e^{-(J_{l+1}-J_{l-1})/T} , \end{aligned} \tag{31}$$

respectively. Then using these expressions and expanding Eq. (30) to lowest order, in exponential terms in T, we find that for the case of a $(\Gamma_1+\Gamma_2)$ cluster containing between 3 and 5 spins Eq. (30) has a solution, near $s=0$, of the form

$$s\simeq-\tfrac{1}{2}(e^{-(J_l-J_{l_1})/T}+e^{-(J_l-J_{l_2})/T}) , \tag{32}$$

where $l_1=l-1$ and $l_2=l+1$ for a two-spin $(\Gamma_1+\Gamma_2)$ cluster with J_l the maximum exchange in the cluster, $l_1=l-2$ and $l_2=l+2$ for a five-spin cluster, and $l_1=l-1, l_2=l+2$ or $l_1=l-2, l_2=l+1$ for a four-spin cluster. For larger clusters, the expression for the pole which occurs near $s=0$ is more complicated, involving more than three J's, but it is unlikely that such large clusters will occur, as is evident from Fig. 1.

When substituting Eq. (32) into Eq. (29) we obtain

$$M(t)\sim\prod_k\int\int P(J_k)e^{ts(J_l,J_{l_1},J_{l_2})}ds\,dJ_k , \tag{33}$$

where the product over k extends to the values of k corresponding to a given cell. These types of integrals appear often in the study of metastability in random problems.[20] To see how they are evaluated we rewrite

$$ts(J_l,J_{l_1},J_{l_2})=-\tfrac{1}{2}(e^{-[g_1(J_l,J_{l_1})-A]/T}+e^{-[g_2(J_{l_1},J_{l_2})-A]/T}) .$$

Here g_1 and g_2 are the exponents of the exponentials in Eq. (32) and

$$A=T\ln t .$$

We see that in the low-T limit the two exponentials have two extreme limiting values with a narrow intermediate region in between. If $(g_1,g_2)\ll A$ then $t|s|\gg1$, and when $(g_1,g_2)\gg A$, $t|s|\ll1$. Thus we can approximate

$$e^{st}\simeq\Theta(g_1-A)\Theta(g_2-A) .$$

This facilitates the evaluation of the integrals considerably. Physically, this approximation means that metastable states with barriers larger than A cannot decay, whereas those with barriers smaller than A can decay and therefore contribute to $M(t)$. The integrals in Eq. (33) can then be evaluated explicitly. Care has to be taken with regard to the singularities in $P(J)$. The integrals in Eq. (33), valid in the SG and F cases, are of the same form as those obtained previously for the AF case.[12] This implies that the remanence found in the SG and F cases is also due to the existence of Γ clusters in these models. Of course, quantitatively they are different, i.e., there is more remanence for the F than for the

SG cases and less for the AF model, as will be seen in the next section. A direct analytic evaluation of the proportionality constant in Eq. (33) is, however, beyond the scope of this paper. Using the step-function approximation plus the explicit form for s given in Eq. (32), we obtain the remanent magnetization as[12]

$$M(t)\sim\frac{1}{3}-\frac{2(1-\alpha)^3}{2-3\alpha}A+\frac{(1-\alpha)^2(1-2\alpha)}{1-3\alpha}A^2-\frac{\Gamma(2-\alpha)\Gamma(3-2\alpha)}{(3-4\sin^2\pi\alpha)\Gamma(4-3\alpha)}A^{3(i-\alpha)}.$$

This result is valid for $\alpha\neq\frac{1}{3},\frac{2}{3}$. For these values an explicit expansion in A gives the appropriate convergent answers.[12] The explicit expansion for $M(t)$ given above represents one of the central results of this paper. The decay of $M(t)$ to zero is not surprising for a one-dimensional model. The difference from the nonrandom problem is that the decay is nonexponential. We can think of this as the existence of a spectrum of relaxation times. In this section we have found that there is remanence in the three cases considered, AF, F, and SG. Kumar and Stein[9] have also studied the characteristic time decay of the magnetization for the SG and F cases with uniform probability laws. Their method of analysis uses the continued-fraction approach numerically. They find that there is a $T\ln t$-type decay to M_r. This agrees with the leading contribution to our analytic calculation taking $\alpha=0$.

An apparent point of disagreement between their results and ours is that they interpret their numerical results as saying that $M_r=0$ for all $T>0$ in the F case. As we have seen above, and also shown by the Monte Carlo calculations of the hysteresis loops of Sec. IV, there is metastability also in the F case. The appearance of remanence in our analysis is related to the $s=0$ pole in the continued fraction. From looking at Fig. 6 in Ref. 9 we seem to see also that the density of states has a pole $s=0$, at the lowest temperatures considered. It is possible that our results are valid only in the $T\to0$ limit, which may be outside of the range considered by Kumar and Stein.

D. Intermediate temperature regime

In this regime the equation of motion (2) can be written as

$$\dot{q}_i=-q_i+\gamma_i q_{i+1}+\gamma_{i-1}q_{i-1}+O(\gamma^3)\ , \tag{34}$$

where we have defined

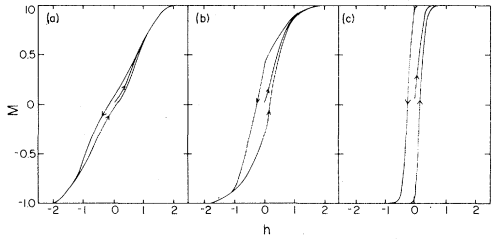

FIG. 6. $T=0.1$ hysteresis curves for: (a) antiferromagnet, (b) spin glass, and (c) ferromagnet, generated by the Monte Carlo technique described in the text. The same 501 spin lattice was used for the calculations with only the signs of the couplings changed appropriately. The arrows indicate the direction in which the field is changing along the curves.

$$\gamma_i=\tanh J_i/T\ . \tag{35}$$

Here γ is always smaller than one. Then Eq. (34) is a good approximation to the equation of motion (2) at intermediate temperatures, where the correlation between the J's is negligible. When the temperature is high enough such that $\{\gamma\}\simeq0$, the dynamics are purely diffusive, characteristic of independent Ising spins.

In this form, the equation of motion is analogous to the equation of motion resulting from a tight-binding Hamiltonian with off-diagonal disorder. Most studies of this problem have centered on the behavior of the density of states at the center of the band. Theodorou and Cohen[21] first found that the density of states diverges at the center of the band. A more detailed study of this divergence was given by Eggarter and Riedinger.[22] In order to see if the divergence has consequences in our problem we calculate the configurationally averaged on-site magnetization. Following ER we define

$$\Delta_i=\gamma_{i-1}\tilde{q}_{i-1}(s)/\tilde{q}_i(s)\ . \tag{36}$$

To obtain Eq. (36) we have taken $\{q_i(0)=0\}$ and $\tilde{q}_i(s)$, as before, is the Laplace transform of $q_i(t)$. From the requirement that the evolution of Δ_{2i} be a diffusive type we get the following [see Eq. (18) in ER]:

$$\tilde{q}_{i+1}(s)=O(\gamma_i,\gamma_{i+1})\tilde{q}_i(s)\ , \tag{37}$$

where

$$O(\gamma_i,\gamma_{i+1})=\gamma_i/[\epsilon/2+\tfrac{1}{2}(\epsilon^2-4\gamma_{i+1}^2)^{1/2}]\ , \tag{38}$$

The solution of Eq. (37) averaged over the J's is

$$[\tilde{q}_i(s)]_J=\prod_j^i[O(\gamma_i,\gamma_{j+1})]_J\ . \tag{39}$$

Here we have assumed that $q_0(t)$ is frozen to only one value $q_0(t)=1$. The configurational average in Eq. (39) is not easy to carry out because of the correlation between the different $\gamma_i's$ in Eq. (38). However, at sufficiently high temperatures, such that $\gamma_i \approx J_i/T$, the configurational averages can be carried out giving

$$[q_n(s)]_J \sim e^{-n \ln T\epsilon + O(n/\epsilon T^2)} . \quad (40)$$

This result has been obtained in the limit of high temperatures. The leading term in Eq. (40) is independent of the particular form of $P(J)$ but the corrections are dependent on its form, as well as the proportionality constant that depends on $(J)_J$. A "dynamic" correction length can then be defined as

$$\xi_D^{-1} = \ln T\epsilon , \quad (41)$$

which can be added to the different types of correlation lengths we defined in Sec. II. The form of the leading term in Eq. (39) is directly integrable and leads to an essentially exponential decay with time for $[q_i(t)]_J$, together with its exponential decay in space. It should be pointed out that the result in Eq. (40) is independent of the signs in the J's insofar as the form of the diffusion equation for the Δ's is dependent only on γ^2.

From this result we see that the singularity in the density of states, which is related to the form of ξ_D, does not have a physically significant influence in the magnetization. Although we have only calculated the decay on space and time of the single site $q_i(t)$, it is easy to see that similar results are obtained for the total magnetization.

IV. MONTE CARLO SIMULATION OF DYNAMICS

In order to strengthen our belief in the results of Sec. III, as well as to further our understanding of these models, we have carried out a Metropolis simulation of the time-dependent properties of these models. This method allows us as well to calculate other quantities harder to estimate analytically. Our method follows the standard procedure (see Binder[23]): We select spins at random, allowing them to flip. If the energy change ΔE is smaller than zero the flip is accepted. If $\Delta E \geq 0$ the flip is accepted only if $\exp[-(\Delta E/T)] \geq X$, with X a uniformly distributed random number between zero and one.[24]

The lattices used in the MC simulations have the same set of J's used in Sec. II. The calculations were done for $N=501$, 1001, and 2001 with small differences in the results. Thus most of the results presented here correspond to a $N=501$ spins lattice.

Rather than wait for the system to reach equilibrium, we required nearest-neighbor spins to satisfy the exact correlation function in equilibrium,[14]

$$\langle S_i S_{i+1} \rangle = -\tanh J_i/T .$$

As we saw in Sec. III at $T=0$ the model has metastable states that are independent of the form of $P(J)$, provided $P(J)$ is continuous. When the temperature is increased the particular form of decay for the remanent magnetization depends on $P(J)$ essentially for values of $\alpha \geq 0.5$. In Fig. 6 we show the hysteresis curves for $\alpha=0.3$, in the AF, F, and SG cases. As expected the widest hysteresis loop corresponds to the F case followed by the SG and AF cases, respectively. The width of the hysteresis loops decreases as T increases, as expected (Fig. 7). This is related to the smaller energy barriers, to flip whole clusters of spins, with respect to the thermal energy. These calculations were done isothermally as follows: The system is started in equilibrium at $h=0$. The field was then increased by 0.1 every 600 MCS/spin (Monte Carlo steps per spin). The average magnetization of the new field was calculated by averaging over the time the field was on. This process was continued until saturation was reached. Then the field was decreased by 0.1 every 1×10^3 MCS/spin, until saturation occurred in the opposite direction. Finally the procedure was reversed.

Next we turn to the calculation of the remanent magnetization. We started with the sample at high temperatures in the presence of a magnetic field. The temperature is lowered until the desired temperature is reached. At this point the field is turned off and the system is allowed to relax at zero field and fixed temperature. This magnetization is known to experimentalists as thermoremanent magnetization. Our specific calculations started at $T=10$ in the presence of a desired field. The system was cooled with $\Delta T=1$ every 1×10^3 MCS/spin for $T>1$. Below $T=1$ the cooling is done at a $\Delta T=0.1$ rate every 1×10^3 MCS/spin until the final temperature is reached. After the field

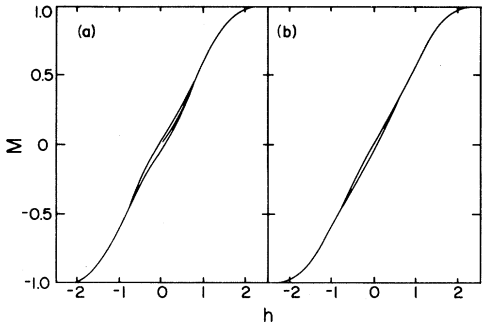

FIG. 7. Antiferromagnetic hysteresis curves for (a) $T=0.2$ and (b) $T=0.3$. The lattice used here is the same one used in Fig. 6.

is off we save the spin configurations for future reference. The system is left to evolve for another 1×10^3 MCS/spin. Averages are taken of M every 40 MCS/spin starting after 60 MCS/spin (corresponding to the fast decay). This procedure is repeated 19 times and the average value of M, with its standard deviations, typically look as in Fig. 8, for $\alpha=0.3$ with final temperature $T=0.05$ and $h=0.5$, 1.25, and 1.85. Note that at low initial fields the remanence is of the order of 0.08 per spin, while at larger fields it decreases towards zero. In fact, when the initial state had all the spins oriented in one direction M_r was essentially zero in agreement with the continued-fraction argument of Sec. III.

Our MC simulations were made in the range $T=0.05$–0.5 for $\alpha=0.3$, with initial fields $n=0.5$, 1.25, and 1.85. As expected large α calculations reduce the remanence and are therefore more difficult to study numerically. This made it difficult to extract the $A^{3(1-\alpha)}$ contribution to M_r for $\alpha\geq0.7$. For $\alpha=0.3$ the remanence is larger and it decays consistent with a $T\ln t$ behavior. However, again, because of the error bars a quantitative comparison was not attempted. Essentially the MC calculation shows qualitatively the trends expected from our detailed analysis. In Fig. 9 the behavior of M_r, after the initial exponential decay, is shown for different values of α vs $T\ln t$.

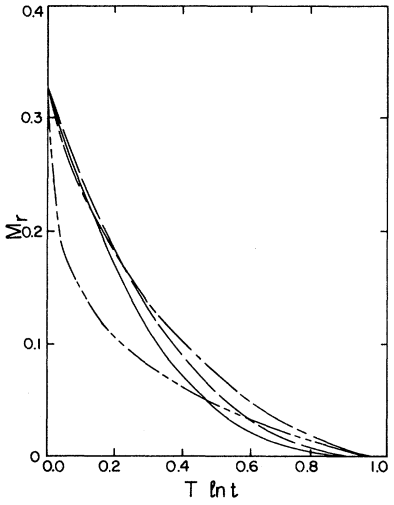

FIG. 8. Time-dependent behavior of the remanent magnetization after the initial exponential decay vs $T\ln t$. We have factored out the unknown prefactor multiplying the magnetization, which depends upon the preparation of the samples. The value of α for the different curves is the one given in Fig. 2.

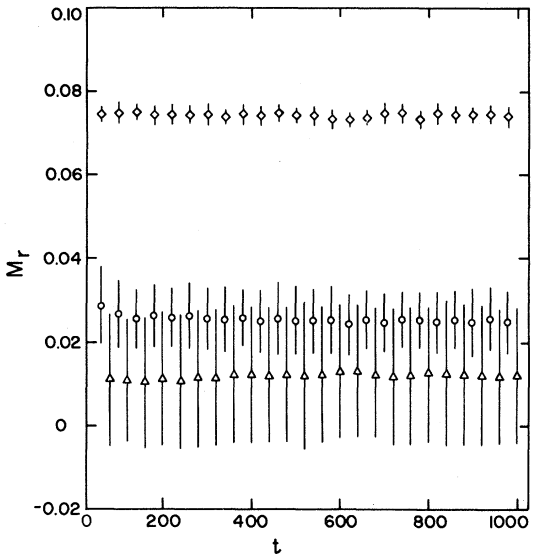

FIG. 9. Thermoremanent magnetization $t=0$ corresponds to the instant $h=0$. The error bars measure one standard deviation in the data (20 runs for each value of h). All three experiments were conducted at $T=0.05$ with initial magnetization fields: (a) 0.5 (diamonds), (b) 1.25 (circles), and (c) 1.85 (triangles). For the sake of clarity the $h=1.85$ points have been set 20 MCS/spin to the right of their true positions.

V. CONCLUSIONS

We have presented a comprehensive study of the thermodynamic and dynamic properties of random Ising chains. This included the spin-glass and the ferro- and antiferromagnetic cases. The analysis was done using different numerical and analytic techniques, to consider arbitrary ranges of temperature and an external magnetic field applied. The results are mostly dependent on the probability law $P(J)$ used. The form of $P(J)$ was chosen on physical grounds to be singular. Also, we took $P(J)$ singular to simulate, to some extent, the asymptotic fixed-point probability law derived in the studies of the AF Heisenberg $S=\frac{1}{2}$ model. From our static results we see that the susceptibility at low temperatures is singular in all three cases but only in the AF and F cases is it nonuniversal, i.e., dependent on $P(J)$. Insofar as the dynamics properties are concerned our main result is that the two-time decay previously found in the SG case also takes place in the AF and F cases. Previously, however, from a numerical continued-fraction study of the F case it was believed that no remanence appears in this case.[9] At low temperatures, where the appearance of remanence is dominant, we calculated analytically, starting from Glauber's equation of motion, the remanent magnetization. Adding a magnetic field complicates the study of the equation of motion analytically. Thus we have calculated the hysteretic properties of the three cases using the METROPOLIS

sampling technique. There it is seen clearly that the remanence is larger in the ferromagnetic and smallest in the AF case.

The appearance of remanence in Ising models is traced down to the existence of a new type of clusters called Γ clusters. These clusters have the property that the magnitude of the exchange constants within a cluster have to be in ascending or descending order. When the J's are all of the same value within a cluster the contribution to the remanence is zero. This explains why the discrete probability laws lead to very different properties to continuum probability laws in Ising systems.

Although the appearance of the Γ clusters seems to be exclusive to Ising model systems, the appearance of remanence may be a general property of random chains. In Ref. 12 we have pointed out the similarity of our results for the AF case and the experiments in $Qn(TCNQ)_2$. There, a Heisenberg $S=\frac{1}{2}$ model is believed to be the relevant model. A two-time decay for the recovery magnetization is observed that is similar to the one found here. This behavior is seen at relatively low temperatures ($\lesssim 0.1$ K), such that a small ion anisotropy could drive the spins into Ising-type configurations. Further experiments are needed to find out if the two-time decay seen in $Qn(TCNQ)_2$ is related to remanence effects.

ACKNOWLEDGMENTS

One of us (J.V.J) has been supported by a Research and Development grant at Northeastern University and also by NSF Grant No. DMR-8114848. One of us (M.M.) acknowledges support from the National Science Foundation Grant No. DE-AC02-81 ER10866 and another of us (J.S.) acknowledges support from the Department of Energy Contract No. 8370.

---

†Present address: Dept. of Physics and Astronomy, University of Maryland, 20742.

*Present address.

[1]See, for instance, the review talk by G. W. Clark, *International Conference in One Dimensional Systems,* edited by J. Bernasconi and T. Schneider (Springer, Berlin, 1981), p. 289.

[2]J. Hirsch and J. V. José, J. Phys. C 13, L53 (1980); Phys. Rev. B 22, 5339 (1980); in Ref. 1, p. 302.

[3]S. K. Ma, C. Dasgupta, and K. Hu, Phys. Rev. Lett. 43, 1434 (1979); C. Dasgupta and S. K. Ma, Phys. Rev. B 22, 1305 (1980).

[4]Z. G. Soos and S. R. Bondeson, Solid State Commun. 35, 11 (1980); Phys. Rev. B 22, 130 (1980).

[5]J. Hirsch, Phys. Rev. B 22, 5355 (1980); J. Chalupa, Solid State Commun. 38, 511 (1981).

[6]S. Alexander, J. Bernasconi, W. Scheider, and R. Orbach, Rev. Mod. Phys. 53, 175 (1981).

[7]R. Glauber, J. Math Phys. 4, 294 (1963).

[8]G. Theodorou and M. Cohen, Phys. Rev. B 19, 1561 (1979).

[9]D. Kumar and J. Stein, J. Phys. C 13, 3011 (1980).

[10]L. C. Tippie and G. W. Clark, Phys. Rev. B 23, 5854 (1981).

[11]J. V. José, M. Mehl, and J. Sokoloff, Proceedings of the International Conference on Low-Temperature Physics [Physica B + C 108, 1375 (1981)].

[12]J. V. José, M. Mehl and J. Sokoloff, Phys. Rev. B 25, 2026 (1982).

[13]H. E. Stanley, *Introduction to Phase Transition* (Oxford University, New York, 1971).

[14]J. Fernandez and R. Medina, Phys. Rev. B 19, 3561 (1979).

[15]P. W. Anderson, D. J. Thouless, E. Abrahams, and D. Fisher, Phys. Rev. B 22, 3519 (1980).

[16]B. Derrida and H. Hilhorst, J. Phys. C 14, L5391 (1981).

[17]G. Grinstein, A. N. Berker, J. Chalupa, and M. Wortis, Phys. Rev. Lett. 32, 1508 (1976).

[18]S. Kirkpatrick, Phys. Rev. B 16, 1630 (1977).

[19]G. Czycholl and B. Kramer, Z. Phys. B 39, 193, (1980).

[20]S. K. Ma, Phys. Rev. B 22, 4484 (1980).

[21]G. Theodorou and M. Cohen, Phys. Rev. B 10, 4597 (1976).

[22]T. P. Eggarter and R. Riedinger, Phys. Rev. B 18, 569 (1978).

[23]K. Binder, J. Phys. (Paris) Colloq. 6, C6-1527 (1976).

[24]We have chosen to simulate the model by the METROPOLIS method instead of the Glauber equation (20), because it is believed that the differences between both ways is quantitatively small [E. Stoll, K. Binder, and T. Scheider, Phys. Rev. B 8, 3266 (1973)].